

Far Field Investigations on Quantum Cascade Lasers

S. Schartner, M. Austerer, M. Nobile, S. Golka A. M. Andrews, W. Schrenk, G. Strasser

Zentrum für Mikro- und Nanostrukturen, TU Wien,
Floragasse 7, A-1040 Wien

Introduction

Quantum cascade lasers (QCLs) are unipolar semiconductor lasers operating in the mid infrared region. Their emitted wavelength is defined by the separation of intersubband levels which can be tailored by band structure engineering. Due to the fact that the maximum conduction band offset in the GaAs/AlGaAs material system is 380 meV, the lowest directly accessible wavelength is roughly 7 μm . One way to reach lower wavelengths is to use intracavity nonlinearities. With sum frequency (SF) generation or second harmonic (SH) generation respectively it is possible to cover the spectroscopically important band between 3.5 μm and 7 μm . Unlike conventional interband semiconductor lasers QCLs do not suffer from the problem of strong absorption of the frequency doubled light because the emission energies (100 – 300 meV) are well below the band gap of the hosting GaAs ($E_{\text{Gap}} = 1.4 \text{ eV}$).

Although GaAs has a nonzero second-order susceptibility, there is no resulting second-order polarization for standard QCLs. This is due to the selection rules for intersubband transitions which allow gain only for TM polarized light, which in turn due to crystal symmetry together with the typical $\langle 100 \rangle$ growth direction cannot excite nonlinear polarization in the host material. However it was shown that QCLs grown on $\langle 111 \rangle$ substrates show sum-frequency generation due to bulk nonlinearity [1]. In our approach we instead use active region designs that include a nonlinear cascade [2], [3]. These artificial nonlinear susceptibilities can reach values comparable to those for the bulk material. The principle of nonlinear light generation in QCLs was actually firstly demonstrated using this intersubband approach in 2003 with the InP material system [4].

Another very interesting topic is intracavity difference-frequency generation in QCLs. It could eventually be used to generate coherent THz radiation in a semiconductor laser at room temperature. Recently THz sideband generation from a THz QCL and a near-infrared diode laser has been shown [5].

An important issue with intracavity SH generation is the optimization of the waveguide for both fundamental and SH frequencies. We show how a double AlGaAs waveguide helps to improve the conversion efficiency compared to a conventional double-plasmon waveguide as used in GaAs based QCLs. We present farfield measurements of the fundamental laser mode and the SH emission that will help investigating modal phase-matching conditions.

Waveguide Design

The nonlinear susceptibility itself is optimized by means of band structure engineering. The external linear to nonlinear conversion efficiency however depends additionally on the waveguide used. Issues like losses, modal overlap and phase-matching have to be

considered. Originally the nonlinear active regions were all embedded in a symmetric double-plasmon waveguide that consists of a low-doped core region (GaAs, $n_{\text{Si}} = 3 \times 10^{16} \text{ cm}^{-3}$) and highly-doped cladding layers (GaAs, $n_{\text{Si}} = 4 \times 10^{18} \text{ cm}^{-3}$) (compare Fig. 1(a)). This waveguide is optimized for fundamental laser action using the dramatic drop in refractive index near the plasma frequency for confinement. However, the strong dispersion near the plasma frequency cannot provide satisfactory confinement for the fundamental and SH radiation at the same time. Figure 1(b) is illustrating this fact: a doping level leading to a refractive index sufficient to confine the fundamental mode does not yield in a sufficiently low refractive index for the SH mode. The calculated refractive index for the $\sim 5 \mu\text{m}$ light in the active region is 3.24, whereas it is only 3.14 in the cladding layers. This results in low confinement of the frequency doubled light. Hence, the losses are high, the overlap to the active region is poor and so is the overlap with the fundamental mode. Additionally the refractive indices of the fundamental and the SH light differ strongly and phase-matching cannot be achieved using this kind of waveguide.

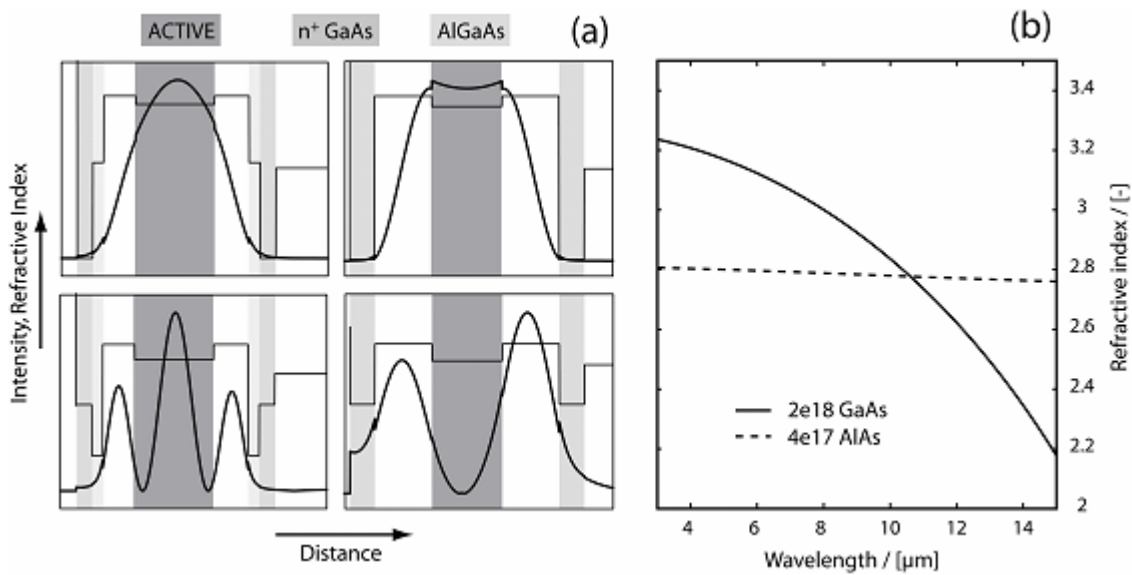


Fig. 1: (a) Mode profiles of the fundamental (upper) and SH (lower) and the line up of the real part of the refractive index are shown for a double-plasmon (right) and a double-AlGaAs (left) waveguide. The combination of a medium doped AlGaAs and a highly doped GaAs layer provides good confinement for both frequencies. (b) The real part of the refractive index calculated with the Drude model for n^+ GaAs and n AlAs.

A waveguide design which substitutes part of the plasmonic cladding with highly Al containing layers can help with these problems. As shown in Fig. 1(a) the fundamental mode is still confined by the thinner n^+ GaAs layer but with support from the AlGaAs spacers. This can even decrease the losses due to the reduced free carrier absorption. However, for the SH mode the AlGaAs actually plays the role of a cladding layer.

Two devices were grown and processed to Fabry-Perot lasers. A bound-to-continuum active region design was embedded in a double $\text{Al}_{0.9}\text{Ga}_{0.1}\text{As}$ waveguide ($n_{(5\mu\text{m})} = 2.86$). The layer sequences are $0.3 \mu\text{m}$ GaAs ($n_{\text{Si}} = 4 \times 10^{18} \text{ cm}^{-3}$), $0.7 \mu\text{m}$ $\text{Al}_{0.9}\text{Ga}_{0.1}\text{As}$ ($n_{\text{S}} = 2.4 \times 10^{17} \text{ cm}^{-3}$), $2 \mu\text{m}$ GaAs ($n_{\text{Si}} = 4 \times 10^{16} \text{ cm}^{-3}$), 60 cascades of bound-to-continuum active cells, $2.2 \mu\text{m}$ GaAs ($n_{\text{Si}} = 4 \times 10^{16} \text{ cm}^{-3}$), $0.7 \mu\text{m}$ $\text{Al}_{0.9}\text{Ga}_{0.1}\text{As}$ ($n_{\text{Si}} = 2.4 \times 10^{17} \text{ cm}^{-3}$), $1 \mu\text{m}$ GaAs ($n_{\text{Si}} = 4 \times 10^{18} \text{ cm}^{-3}$) and n -type GaAs substrate. For this structure we calculate refractive effective indices of 3.185 (fundamental, TM_{00}) and 3.181 (nonlinear light,

TM_{02}). This was calculated for an infinitely wide laser ridge. Using a SiN_x insulation and gold at the side walls, a ridge width dependent fine tuning of the refractive index is possible and phase matching is calculated to occur for laser ridges around $25 \mu m$ thickness. This structure further strongly increases the confinement factor, especially for the nonlinear light, where it is increased from 17% to 65%. Besides the improvement in confinement, this waveguide also enhances the overlap of fundamental and nonlinear light.

Results

Depending on the ridge width we were able to increase the conversion efficiency from approximately 15 to $100 \mu W/W^2$ and achieve nonlinear peak powers exceeding $100 \mu W$. This improved performance is due to a higher confinement and lower losses for the SH light. According to our calculations the overall refractive index difference between the fundamental and SH is also reduced, and it might be possible to achieve modal phase matching in such a waveguide. As shown in Fig. 2 we observe a maximum conversion efficiency of $120 \mu W/W^2$ for $30 \mu m$ wide devices.

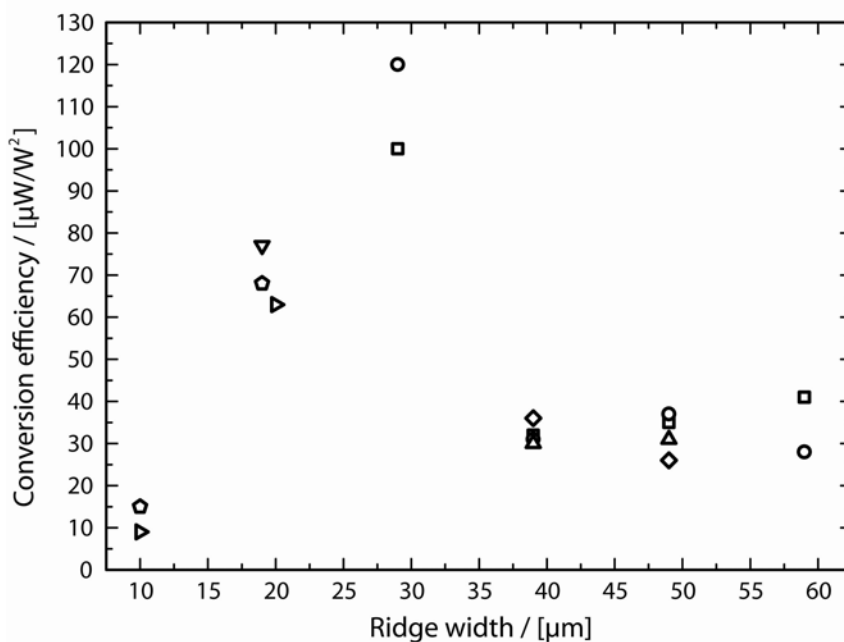


Fig. 2: Conversion efficiencies for lasers of different ridge widths. The conversion efficiency increases starting from thin ridges and falls again after it reaches a maximum around $30 \mu m$. Modal phase matching is calculated to occur for $25 \mu m$ wide laser cavities.

To investigate the mode profiles in the laser waveguide we were analyzing their farfields. Fig. 3(a) shows a typical farfield profile of a TM_{00} mode which we observed up to ridge widths of $60 \mu m$ for the fundamental light. We attribute this to the lossy SiN_x insulation layer which suppresses higher-order lateral modes. This in turn is not the case for the SH radiation as the waveguide dimensions are roughly scaled by a factor of two, and the SiN_x losses are lower. The two-fold pattern of the SH farfield (Fig. 3(b)) in lateral direction can therefore be explained by a higher-order lateral mode. In growth direction the farfield is split in three lobes of comparable intensity. This pattern cannot be

explained by solely one TM_{02} mode, but rather suggests a superposition of at least two modes (TM_{00} and TM_{02}).

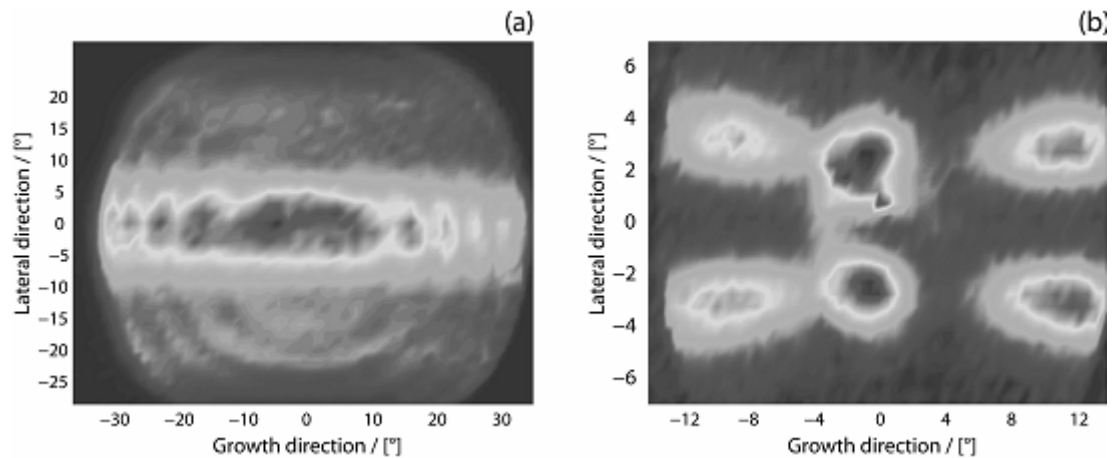


Fig. 3: Farfield profiles of the fundamental (a) and SH (b) modes for a 40 μm wide Fabry-Perot device with double AlGaAs waveguide. The plots were recorded at distances of 100 mm and 50 mm respectively.

Conclusion

We have shown that second-harmonic and sum-frequency emission in GaAs based QCLs grown on $\langle 100 \rangle$ substrates can be significantly enhanced with a double AlGaAs waveguide. In order to fully exploit the nonlinear properties of GaAs based QCL structures, appropriate waveguide designs that enable phase matching have to be developed. To reach this goal we performed farfield measurements that allow us insight into the SH modal behavior. Future goals include further enhancement of SH generation and the demonstration of difference-frequency generation.

References

- [1] J.-Y. Bengloan *et al.*, *Appl. Phys. Lett.* 84, 2019 (2004)
- [2] C. Pflügl *et al.*, *Electron. Lett.* 41, 1331 (2005)
- [3] C. Pflügl *et al.*, *Appl. Phys. B* 85, 231 (2006)
- [4] N. Owschimikow *et al.*, *Phys. Rev. Lett.* 90, 043902 (2003)
- [5] S.S. Dhillon *et al.*, *Appl. Phys. Lett.* 87, 071101 (2005)